COMPARATIVE EVALUATION OF METHODS OF ARC AND HYBRID PLASMA-ARC WELDING OF ALUMINUM ALLOY 1561 USING CONSUMABLE ELECTRODE

V.N. KORZHIK[1,2], **N.A. PASHCHIN**[2], **O.L. MIKHODUJ**[2], **A.A. GRINYUK**[2],
A.A. BABICH[1,2] and **V.Yu. KHASKIN**[1,2]

[1]Guangdong Welding Institute (E.O. Paton Chinese-Ukrainian Institute of Welding), Guangzhou, PRC
[2]E.O. Paton Electric Welding Institute, NASU
11 Kazimir Malevich Str., 03680, Kiev, Ukraine. E-mail: office@paton.kiev.ua

In addition to the traditional pulsed arc welding using consumable electrode at reverse polarity, it is advisable to apply hybrid plasma-arc welding using consumable electrode to increase the service life and reliability of welded structures of aluminum alloys. The works on determination of technological modes of hybrid plasma-arc welding of aluminum alloy 1561 of 5 mm thickness and the comparison of the processes of traditional consumable electrode arc welding and hybrid plasma-arc welding, taking into account the residual stress-strain state of the resulting butt welded joints, as well as evaluation of the prospects for replacement of traditional arc welding by hybrid one were carried out. During determination of technological modes of hybrid plasma-arc and pulsed arc welding of the aluminum alloy 1561, it was found that at the same speeds the both methods provide approximately equal energy input. At the same time the mastered technology of hybrid welding provided the reduction in the wire diameter from 1.6 to 1.2 mm, which resulted in 25–50 % smaller width of the weld as compared to arc welding. Reduction in the area of the weld facial part as compared to the root part area in the hybrid welding method led to approximately 3 times decrease in the level of residual distortion of welded plates, and 15–20 % decrease in residual stresses along the weld line. 6 Ref., 1 Table, 10 Figures.

Keywords: aluminum alloy, consumable electrode arc welding, hybrid plasma-arc welding, modes, speckle-interferometry, stress-strain state

Thin-sheet welded structures of alloys on aluminum base find the more and more spreading in modern industry [1]. Such structures are widely applied in aerospace engineering, shipbuilding, automotive industry, railway transport, etc. [2]. In manufacture of structures and products of aluminum alloys, different welding technologies are used to provide the quality formation of permanent joints, for example, pulsed arc welding using consumable electrode at the reverse polarity (further — arc welding). However, in a number of cases (for example, to increase the service life and reliability of welded structures) it is advisable to use more advanced technologies. They include the hybrid plasma-arc welding using consumable electrode with an axial electrode wire feed through the tube electrode of the plasmatron (further — hybrid plasma-arc welding) [3].

The aim of this work is to determine technological modes of hybrid plasma-arc welding of aluminum alloy 1561 of thickness $\delta = 5$ mm, to compare the traditional consumable electrode arc welding processes and hybrid plasma-arc welding taking into account the residual stress-strain state of the produced butt joints, as well as to evaluate prospects of replacing traditional arc welding by the hybrid one.

The mastering of technological methods of hybrid plasma-arc and arc welding was performed on the plates of aluminum alloy 1561 of 320×102.5 mm size. At the same time, the special complex of equipment was applied designed at the E.O. Paton Electric Welding Institute [4]: inverter welding power source for argon-arc welding using non-consumable electrode TIGAC-DCE-VO 450/ TRobot, plasma module FPM, EVOSpeedStar 520 TSRobot, units of autonomous cooling, plasmatron for machine hybrid plasma-arc welding using consumable electrode with an axial wire feed, multiposition laboratory manipulator based on welding column and rotator, common system for the control of hybrid welding complex. Welding was carried out according to the technological scheme shown in Figure 1.

In the course of experiments the longitudinal butt welds were produced on the long side of specimens (Figure 2). One of the main criteria for selection of modes for welding specimens of alloy 1561 was the quality formation of welds the accompanying minimization of pore formation. The used welding modes (welding speed v_w, welding current I_a, arc voltage U_a, diameter of welding wire d_w) and geometric characteristics of plates (f_1–f_3 are the longitudinal deflections, Δ_1, Δ_2 are transverse deflections at the beginning and at the end of joint, respectively) are presented in Table. The appearance of macrosections of welded joints is shown in Figure 3. The mastered and tested hybrid welding technology provided the reduction in the wire
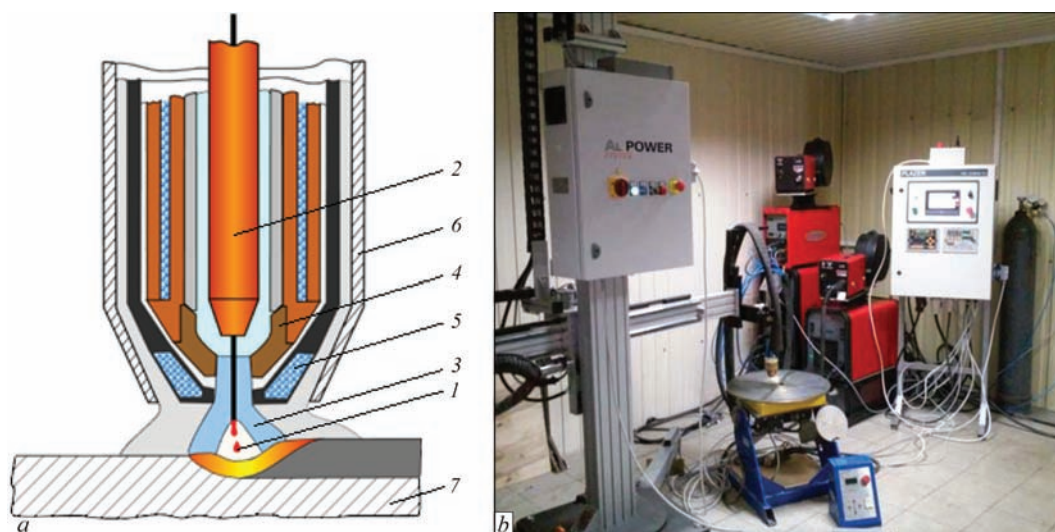
Figure 1. Technological scheme (*a*) and complex of equipment (*b*) for the consumable electrode hybrid plasma-arc welding: *1* — arc of consumable electrode; *2* — feeding tip of consumable electrode; *3* — constricted direct arc; *4* — tubular electrode of plasmatron (anode); *5* — plasma-forming nozzle; *6* — protective nozzle; *7* — specimen being welded

diameter from 1.6 to 1.2 mm at the same thickness of welded plates and the same values of energy input (Table). As far as is shown in [5], the volume of deposited metal is directly proportional to the diameter of electrode wire, thus resulting in a decreased width of the weld at equal welding speeds.

At the selected modes the energy inputs of the compared welding processes are approximately the same and are of the order of 600 J/mm. However, in the case of hybrid plasma-arc welding the welds have a width which is (as compared to the traditional arc): by 25 % smaller along the weld reinforcement and down to 50 % in its middle section (Figure 3). Moreover, the height of the upper bead reinforcement during hybrid welding is reduced approximately by twice as compared to the similar parameter for arc welding. It is seen from Figure 3 that the longitudinal fillet angle of weld section decreases, and the radius of the weld transition to the base metal, on the contrary, increases. This, in its turn, leads to decrease in the stress concentration factor. It can be assumed that the shape of weld penetration, characteristic for hybrid welding, determines a lower level of residual stress-strain state of butt joints. To check this assumption by the method of electron speckle interferometry, the parameters of stress-strain state of welded plates were measured.

The method is based on the measurement of displacements at elastic unloading of the metal volume at the investigated points on the surface of the specimen, caused by drilling of blind holes with a diameter and depth of 1.0 mm [6]. By comparing the parameters of the stress state and residual shape changing on a specific specimen of welded joint made by arc and hybrid welding, the efficiency of each of the processes was determined from the positions of stress-strain state.

The geometric sizes of the plates welded by arc and hybrid methods, as well as schemes for measurement of residual stresses, are presented in Figure 4. The measurements of longitudinal (along the weld
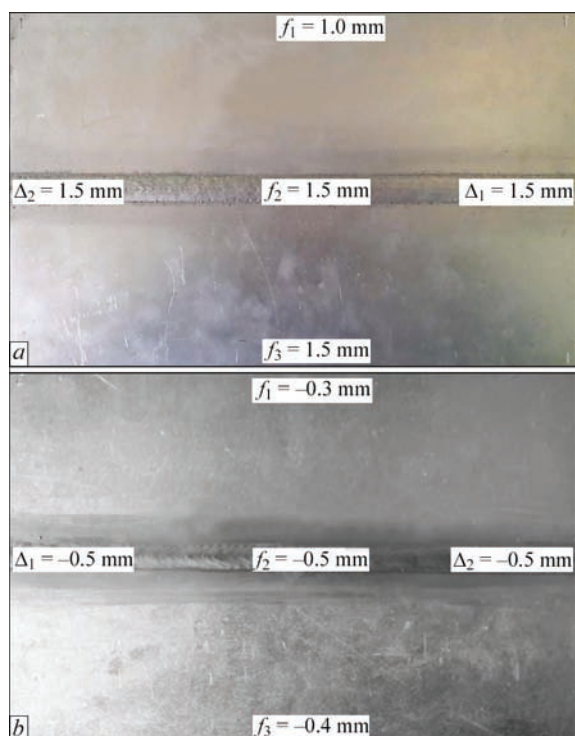
Figure 2. Appearance of facial surface and geometric characteristics of welded joints of alloy 1561 plates made by the arc (*a*) and hybrid plasma-arc welding (*b*)
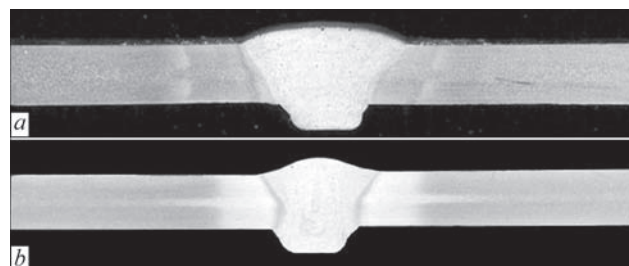
Figure 3. Appearance of macrosections of welded joints of alloy 1561 plates: *a* — arc welding; *b* — hybrid plasma-arc welding

Modes of arc and hybrid plasma-arc welding with close energy inputs (of the order of 600 J/mm) and geometric characteristics of welded alloy 1561 plates ($\delta = 5$ mm)

Type of welding											
MIG						Plasma-MIG					
V_w, mm/s	I_a, A	U_a, V	d_w, mm	$f_1/f_2/f_3$, mm	Δ_1/Δ_2	V_w, mm/s	I_{MIF}/I_{plasma}, A	U_{MIG}/U_{plasma}, V	d_w, mm	$f_1/f_2/f_3$, mm	Δ_1/Δ_2
10	240	26.5	1.6	1.0/1.5/1.2	1.5/1.5	10	145/149	17.4/25.5	1.2	−0.3/−0.5/−0.4	−0.5/−0.5

line) σ_x component of a plane stressed state were performed in three sections $S1$–$S3$ on the facial side of the plate (Figure 4, a) and in one section $S5$ on the back side (Figure 4, b). The duplication of measurements of σ_x on the facial side of the plate was carried out in order to provide the validity of results.

The specimen, made by arc welding (Table, Figures 2, a and 3, a), has longitudinal deflections f_1-f_3 in the range of values 1.0–1.5 mm, directed away from the facial surface. The values of the transverse deflections Δ_1–Δ_2 are stable along the length of welded joint and amount to 1.5 mm. The peculiarities of this forming are determined by the shape of weld penetration (Figure 3, a), characterized by the misalignment of the line of applying shrinkage shortening and a neutral axis of the section. The result of this misalign-

ment is the bending moment, causing distortion of the plate in the longitudinal direction. The stability of the values Δ along the length of the plate is related to its geometric characteristics, providing a uniform heat removal from the surface during welding thermal deformational cycle. The distribution of residual longitudinal stresses σ_x in the cross-sections of welded plate after MIG welding is shown in Figure 5.

It can be seen from Figure 5 that in the weld center on the facial and back surfaces of the plate there is a local decrease in tensile stresses σ_x to 45–50 and 100 MPa, respectively. The peak values σ_x on the facial and back surfaces are located in the fusion zone and reach 100 and 140 MPa, respectively. The reactive compressive stresses σ_x on the facial and back surfaces reach the maximum values −50– −80 and −25– −60 MPa at the longitudinal edges of the plate, respectively. The shape of diagram σ_x is connected with a small width of the plate, at which the compressive stresses in its cross-section do not reach zero values. When comparing the σ_x diagrams on both sides of the plate, one can see that there is a significant bending stress component, which is confirmed by the obtained shape of the specimen distortion.

The distribution of residual longitudinal stresses σ_x in the welded plate along the weld line (Figure 6) confirms the results obtained for the cross-section $S1$ (Figure 5). It can be seen from the Figure that the diagrams σ_x on both sides of the plate are characterized by a difference in peak values, which determines the significant bending component of stress-strain state of the plate and confirms the characteristics of its shape changing.

The specimen, made by hybrid welding (Table, Figure 2, b and 3, b), has longitudinal deflections f_1–f_3 of
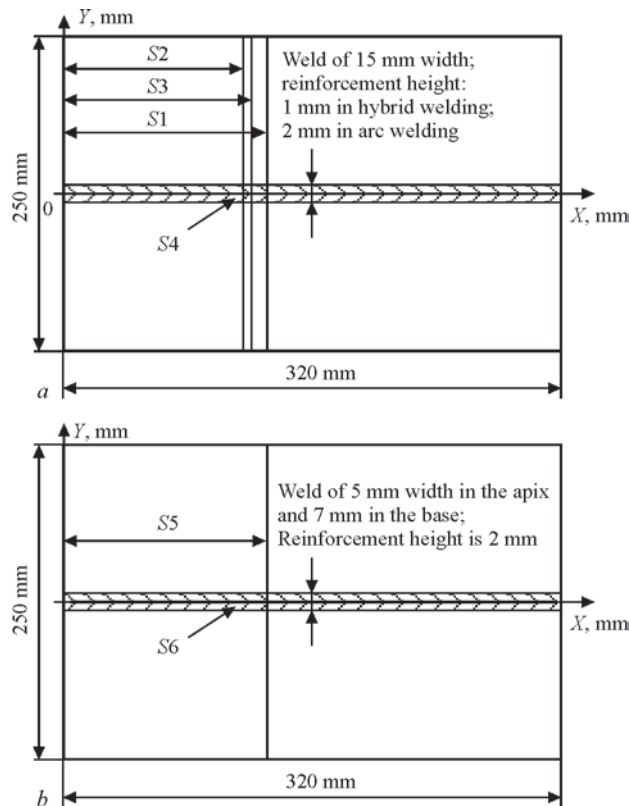
Figure 4. Schemes for measurements of residual stresses on butt welded joints of aluminum alloy 1561, made by arc and hybrid methods: a — facial (*upper*) side, sections $S1$– $S3$ — measurements across the weld, $S4$ — along the weld line; b — back (*bottom*) side, section $S5$ — across the weld, $S6$ — along the weld; along the axis X the sections are located at the distance: $S1$ — 166, $S2$ — 148, $S3$ — 155, $S5$ — 168 mm; along the axis Y the sections $S4$ and $S6$ passed along the zero mark
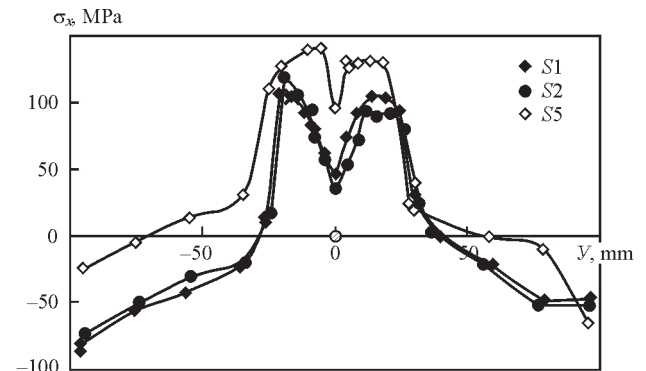
Figure 5. Residual welding stresses σ_x on the facial side of the alloy 1561 joint, made by arc welding, in the cross-sections $S1$ and $S2$ and on the back side — in the section $S5$
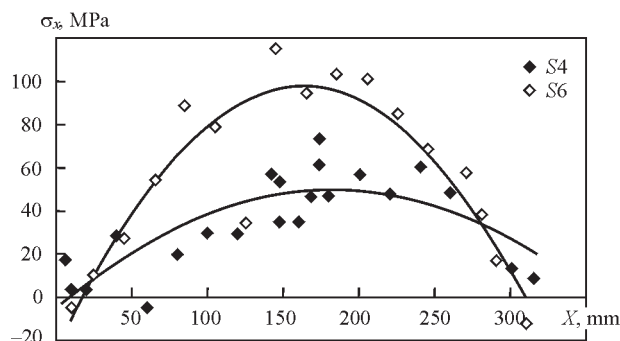
Figure 6. Residual welding stresses σ_x on the facial side of the 1561 alloy joint made by the arc welding in the longitudinal section along the weld line *S4* and the back — in the section *S6*

the value of -0.3–-0.5 mm, directed towards the facial surface. The values of transverse deflections Δ_1–Δ_2 are stable in the length of the welded joint and are also equal to -0.5 mm. The features of this shape changing are determined by the shape of weld penetration (Figure 3, *b*), which is characterized by a practical coincidence of line of applying shrinkage shortening and neutral axis of weld section. A comparison of shapes of welds, produced by arc and hybrid methods (Figure 3), shows that the area of weld section in hybrid welding is by 30 % smaller than that in arc welding.

The plate made by hybrid method is characterized by a smaller volume of longitudinal shrinkage shortening of weld metal and, correspondingly, by a smaller value of longitudinal shrinkage force P_{shs} than the specimen after arc welding. This is connected with a noticeable decrease in the area of the upper relatively horizontal longitudinal axis of the weld part during hybrid welding (Figure 3, *b*) as compared to the arc welding (Figure 3, *a*). Moreover, in both cases, the area of the lower part remains the same. Considering the practical coincidence of the line of applying the longitudinal P_{shr} and longitudinal neutral axis, as well as the smaller value of P_{shr}, it can be concluded that the plate welded in a hybrid method, is subjected to a significantly smaller bending moment than that after arc welding. This fact explains the smaller value (to three times) of the plate distortion in the longitudinal direction than in arc welding. The stability of Δ along the length of the plate, as well as their small values after hybrid welding, are connected with the weld shape, which is characterized by a more uniform penetration (as compared to the arc welding) across the thickness of the plate, and also by geometric characteristics of the specimen, providing a stable heat removal from its surfaces during welding thermal deformational cycle.

The distribution of residual longitudinal stresses σ_x in the cross-sections of facial and back sides of the plate welded by the hybrid method is shown in Figures 7, 8, and their comparison is shown in Figure 9. It can be seen from the Figures that in the weld center on the facial and back surfaces of the plate, there is a local decrease in tensile stresses σ_x to 45–50 and 100 MPa, respectively. The peak values σ_x on the facial and back surfaces are
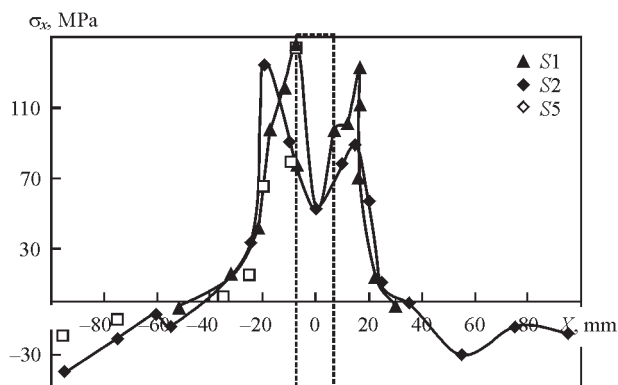
Figure 7. Residual welding stresses σ_x on the facial side of the 1561 alloy joint, made by the hybrid welding, in cross-sections *S1*–*S3*; dashed line shows contours of the weld

located in the fusion zone and reach 140 and 150 MPa, respectively. The reactive compressive stresses σ_x on the facial and back surfaces reach the maximum values of -20–-40 MPa at the longitudinal edges of the plate. This shape of a diagram of compressive stresses σ_x, as in the case of arc welding, is connected with a small width of plate at which the compressive stresses in its cross-section do not reach zero values. Comparing the diagrams σ_x on both sides of the plate, it can be seen that unlike the arc welding, the bending component of stresses in the reactive zone of the stress diagram for hybrid welding is negligible, which determines the smaller value of specimen distortion as compared to the arc method (Table).

It should be noted that analyzing the residual stressed states of plates made by arc and hybrid welding (Figures 5, 9) some discrepancy between the level of tensile stresses and deflection values can be noted. Thus, the peak values of tensile stresses σ_x for the considered welding methods unlike the deflection values, are close enough as well as values of bending stress components in the active zone (in the weld center). This fact can be explained by a small longitudinal rigidity of welded plates being investigated as well as by the features of stress-strain states characteristic for the arc and hybrid welding.

The diagrams σ_x in the reactive zone of compressive stresses reach free longitudinal edges (Figures 5 and 9). At the same time, the stresses at the edges of
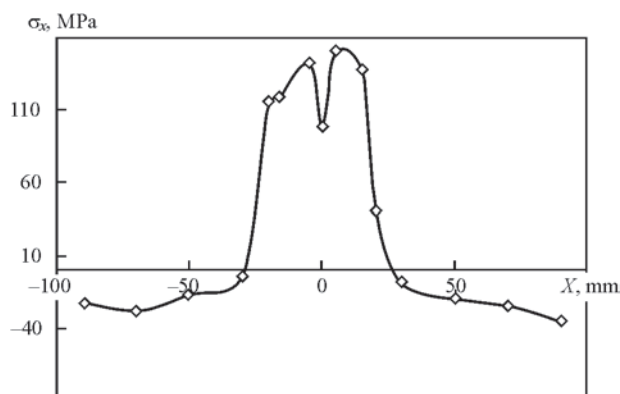
Figure 8. Residual welding stresses σ_x on the back side of the 1561 alloy joint, made by hybrid welding, in cross section *S5*
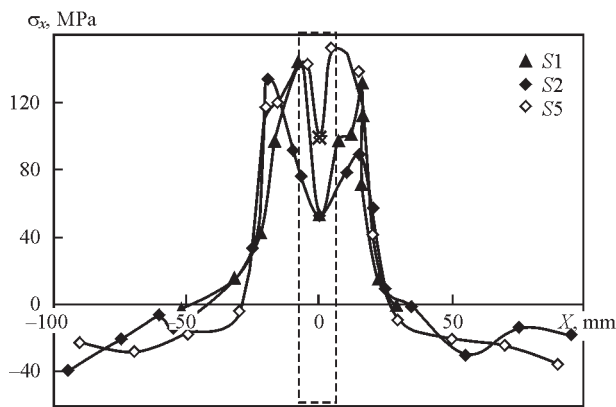
Figure 9. Residual welding stresses σ_x on the facial side of 1561 alloy joint, made by the hybrid welding, in cross-sections $S1$ and $S2$ and on the back side — in section $S5$; dashed line shows weld contours

the plate during hybrid welding are significantly lower than in arc welding, which causes its smaller longitudinal deflections and, correspondingly, a higher level of tensile stresses σ_x. Thus, the level of tensile stresses σ_x in a bent plate welded by arc method, is comparable to the level of σ_x in a plane plate welded by hybrid method. It can be concluded that by comparing the stressed states of the plates made by hybrid and arc welding with equal values of deflections, the values of σ_x in the latter will be higher.

The distribution of residual longitudinal stresses σ_x in the welded plate along the weld line (Figure 10) confirms the results obtained for the cross-section $S1$ (Figure 9). It can be seen from the Figure that the diagrams σ_x on both sides of the plate made by hybrid welding, are characterized by a smaller difference in peak values than in arc welding, which determines the bending component of stress-strain state of the plate and confirms the characteristics of its shape changing (Table).

The comparison of values of the stresses σ_x along the weld line in the plates made by hybrid and arc welding showed 15–20 % decrease in their level in the case of hybrid welding, which can help to increase the service life of such welded joints under the load in this direction. Such an increase in service life of joints, loaded along the weld, can positively affect the results of welding the stringer panels and shells of special aircrafts of aluminum alloys.

Conclusions

1. It was established in the course of determination of technological modes of the hybrid plasma-arc and pulsed arc welding of 1561 aluminum alloy of 5 mm thickness that at the same welding speeds the both methods provide an approximately equal energy input. At the same time, the mastered hybrid welding technology provided the reduction in the diameter of the applied wire from 1.6 to 1.2 mm, which resulted in 25–50 % decreased width of the weld as compared to the arc welding.
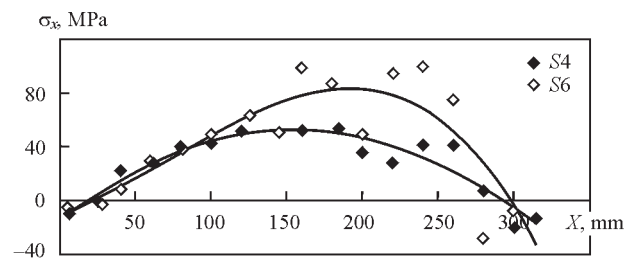
Figure 10. Residual welding stresses σ_x on the facial side of the 1561 alloy joint, made by hybrid welding, in longitudinal section along the line of weld $S4$ and on back side — in section $S6$

2. The reduction in the area of the facial part of the weld as compared to the area of the root part in the hybrid method of welding resulted in approximately 3 times decrease in the level of residual distortion of welded plates, and in 15–20 % decrease of residual stresses σ_x along the weld line.

3 The diagrams of stresses σ_x along the weld line on both sides of the plate being butt welded by the hybrid method, are characterized by a smaller difference in peak values than in arc welding, which determines approximately three times lower bending component of stress-strain state of the plate and is confirmed by the characteristics of its shape changing.

4. The further investigations of stress-strain state of butt joints made by hybrid welding are advisable to be carried out using plates of 500×500×5 mm size, which provide the compressive stresses at the edges close to zero.

1. Khaskin, V.Yu. (2013) Development of laser welding of aluminium alloys at the E.O.Paton Electric Welding Institute (Review). *The Paton Welding J.*, **5**, 51–55.
2. Zusin, V.Ya., Serenko, V.A. (2004) *Welding and surfacing of aluminium and its alloys*. Mariupol: Renata.
3. Grinyuk, A.A., Korzhik, V.N., Shevchenko, V.E. et al. (2015) Main tendencies in development of plasma-arc welding of aluminium alloys. *The Paton Welding J.*, **11**, 31–41.
4. Grinyuk, A.A., Korzhik, V.N., Shevchenko, V.E. et al. (2016) Hybrid technologies of welding aluminium alloys based on consumable electrode arc and constricted arc. *Ibid.*, **5/6**, 98–103.
5. Shonin, V.A., Poklyatsky, A.G. (2001) Low-cycle fatigue of welded butt joints made from alloy AMg6 in inert atmosphere. *Ibid.*, **3**, 18–22.
6. Lobanov, L.M., Pivtorak, V.A., Savitsky, V.V. et al. (2006) Procedure for determination of residual stresses in welded joints and structural elements using electron speckle-interferometry. *Ibid.*, **1**, 24–29.